Bounds on Frequency Response Estimates Derived from Uncertain Step Response Data

John P. Deyst and T. Michael Souders, *Fellow, IEEE*

Abstract— The frequency response of a system can be estimated from measurements of its step response; however, many error sources affect the accuracy of such estimates. This paper investigates the effects of uncertainty in the knowledge of the step response. Methods for establishing uncertainty bounds for the frequency response estimates are developed, based on the corresponding time-domain uncertainties associated with the measured step response. Two methods are described. One method produces bounds that are often very conservative. The other method produces bounds that are more realistic. End effects that influence the bounds are also considered. A simulation example and an application of the bounds are presented.

I. INTRODUCTION

PREVIOUS work has shown that the frequency response of digital oscilloscopes, analog-to-digital converters, and linear systems in general can be effectively estimated from discrete-time step response measurements (e.g., [1]–[7]). Earlier studies have analyzed error sources affecting the frequency response estimates, notably, noise, jitter, aliasing, and derivative estimation errors. However, an obvious and important source of uncertainty—the systematic uncertainty in the knowledge of the step-like waveform—has been neglected. In this paper, we derive uncertainty bounds for frequency response estimates based on the systematic time-domain uncertainty bounds of the measured step waveform. Typically, such bounds are in the form of an uncertainty envelope around the measured waveform, enclosing the "true" waveform. However, an infinite combination of possible error waveforms can exist within a given uncertainty envelope. We propose two methods of producing frequency response uncertainty bounds. The methods utilize the limited information provided by uncertainty envelopes of measured step responses.

A simple method, based on Parseval's Theorem, provides provable upper bounds, but has the disadvantage that it is often overly conservative; i.e., for many time-domain uncertainty envelopes, the Parseval bounds greatly exceed the largest possible frequency-domain errors. The other method, a so-called "envelope-modulation" approach, produces more realistic, provable bounds that can be reached (at least in some pathological cases), but not exceeded.

We also account for errors introduced by "end effects" that occur in the required computations. Finally, we demon-
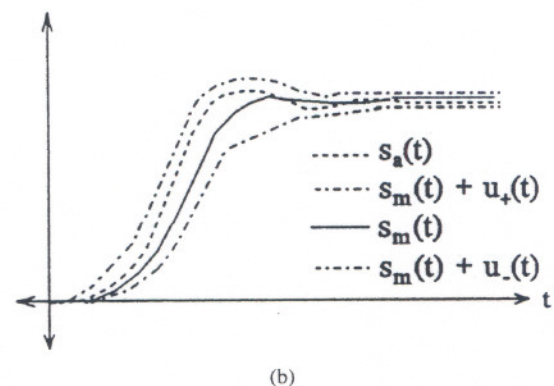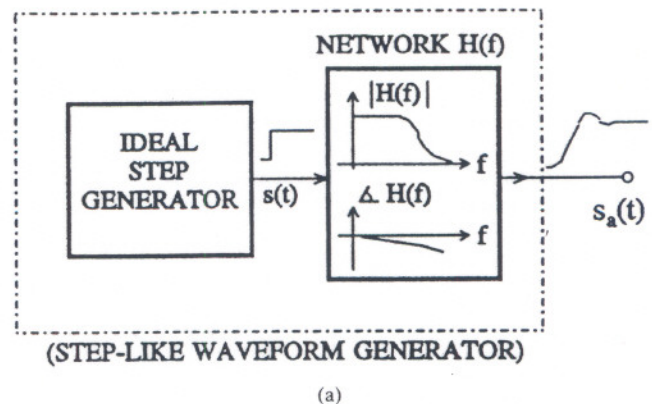
(a)

(b)

Fig. 1. (a) An ideal step source in series with a linear network, $h(t)$; this can model a step-like waveform generator. (b) The circuit produces the waveform $s_a(t) = s(t) * h(t)$, measured to be $s_m(t)$ with uncertainties $u_+(t)$ and $u_-(t)$.

strate their performance with an example, and describe an application.

II. BACKGROUND

Fig. 1(a) shows a source producing an ideal unit step waveform, $s(t)$, that is input to a linear network, producing the step-like waveform $s_a(t)$. The network is characterized by impulse response $h(t)$ and frequency response $H(f)$; $s_a(t)$ is its step response. An ideal step source in series with a linear network can be used as a model for a step-like waveform generator. The network $h(t)$ represents the physical realization of the generator. Such a network model is a useful construct only for certain purposes: while the real, causal, step-like waveform output $s_a(t)$ can always be represented as the result of such a combination, it is unlikely that an actual waveform generator would in fact be a linear system.

The value of $s_a(t)$ is not known exactly, but is estimated by careful measurement to be the waveform $s_m(t)$, with negative and positive uncertainties $u_-(t)$ and $u_+(t)$, respectively. It is assumed here that the uncertainties have been correctly determined such that $s_a(t)$ is between $s_m(t) + u_-(t)$ and $s_m(t) + u_+(t)$, as shown in Fig. 1(b); or equivalently, the measurement error, $e(t)$, is within the uncertainty envelope defined by $u_-(t)$ and $u_+(t)$ for all t values of interest

$$e(t) = s_m(t) - s_a(t) \tag{1}$$

$$s_m(t) + u_-(t) \le s_a(t) \le s_m(t) + u_+(t) \tag{2}$$

$$u_-(t) \le -e(t) \le u_+(t), \quad \text{where} \quad u_-(t) \le 0$$
$$\text{and} \quad u_+(t) \ge 0. \tag{3}$$

[Note the negative sign in front of $e(t)$ in (3), due to the way $e(t)$ is defined in (1).] Determining the uncertainties $u_-(t)$ and $u_+(t)$ correctly, such that they enclose the error with acceptable confidence but are not too large, is a significant problem that we do not venture to solve here; we simply assume that $u_-(t)$ and $u_+(t)$ are correctly determined.

We also assume here that the available data are discrete-time (sampled) versions of $s_m(t)$, $u_-(t)$, and $u_+(t)$

$$s_m[n] = s_m(nT) \tag{4}$$
$$e[n] = e(nT) \tag{5}$$
$$u_+[n] = u_+(nT) \tag{6}$$

and

$$u_-[n] = u_-(nT), \quad \text{for} \quad n = 0, 1, 2, \cdots, (M-1) \tag{7}$$

where T is the sampling interval, n is the sample index, and M is the number of samples in the data record. To avoid spectral leakage errors, the recorded data epoch must have sufficient duration ($M \cdot T$) to allow virtually complete settling of the step-like signal [1]. Since the signals may have frequency components above the Nyquist frequency ($1/2T$), aliasing may have occurred in the sampling process. Uncertainties for aliasing errors have previously been developed [2], [3], and are discussed further below.

Given $s_m[n]$, $u_+[n]$, and $u_-[n]$, we want to estimate the frequency response of the network, $H(f)$, and its magnitude and phase uncertainties. The frequency response $H(f)$ is the continuous-time Fourier transform (CTFT) of $h(t)$, which is the derivative of the step response, $s_a(t)$. $H(f)$ can be estimated from the measured step response data, $s_m[n]$, by a number of methods [1]–[7]; here we apply the method of [2], [3], [7]. The data record $s_m[n]$ is differentiated to obtain a sampled estimate of the impulse response, $h_m[n]$; and then $H_m[k]$, the discrete Fourier transform (DFT) of $h_m[n]$, is computed

$$H_m[k] = \sum_0^{M-1} h_m[n] \cdot \exp\left(\frac{-j2\pi kn}{M}\right). \tag{8}$$

In order to use $H_m[k]$ to estimate values of $H(f)$, it must be normalized by the sampling interval T, as indicated by [8], [9]

$$H_m(f_k) = T(H_m[k]). \tag{9}$$

Note that the DFT produces discrete values, corresponding to certain frequencies f_k

$$f_k = \frac{k}{MT}, \quad \text{for} \quad k = 0, \pm 1, \pm 2, \cdots, \pm\frac{M}{2}. \tag{10}$$

Likewise, the uncertainties of the frequency response estimate are calculated here also just at the discrete frequencies f_k.

If the differentiation of $s_m[n]$ is performed by convolving it with a differentiation filter (e.g., see [10]), then more than M samples of $s_m[n]$ need to be differentiated, to avoid end effects. For example, if the length of the differentiation filter is M_d samples, then at least ($M + M_d$) samples of $s_m[n]$ should be differentiated. After differentiation, at least ($M_d/2$) samples should be removed from both the beginning and the end of the resulting record to reduce end effects, leaving a record M samples long of the impulse response estimate, $h_m[n]$. However, if the differentiation is performed using the first difference operator, only M samples of $s_m[n]$ are needed, if care is taken at the end of the record [2]. Even following this procedure, some end effects will still occur; they are discussed later.

We recommend that the uncertainties $u_+[n]$ and $u_-[n]$ be used to bound only the systematic errors associated with the estimation of $s_a(t)$: e.g., unknown or uncorrected systematic measurement errors. Separately, variances of $H_m[k]$ due to random errors of $s_m[n]$ can be calculated with closed-form solutions, if the usual assumptions are made concerning the statistical properties (e.g., see [2], [3]). Uncertainties due to aliasing and nonidealities of the differentiation of $s_m[n]$ should also be determined separately [2], [3]. The random variance estimates can then be combined with the aliasing and differentiation uncertainties, and with the systematic uncertainties developed here, to arrive at expanded uncertainties for the frequency response estimates [11].

III. BOUND ESTIMATES

The main contribution of this work is providing methods for calculating the uncertainties of the magnitude and phase response estimates, from the time-domain uncertainties of the measured step response. The problem is difficult because there are an infinite number of different possible error signals that can occur within given time-domain uncertainties, each having a different Fourier transform. Two methods to calculate frequency response uncertainties are presented below.

A. Parseval Method

The first method applies Parseval's Theorem to equate the total possible error energy that can be enclosed by the time-domain uncertainties to a maximum possible error energy in the frequency domain. The magnitude response uncertainties for a given frequency are then determined by assuming that all the error energy could be concentrated only at that frequency. For each data sample, find the maximum magnitude, $u_{\max}[n]$, of the uncertainties $u_-[n]$ and $u_+[n]$

$$u_{\max}[n] = \max\left(|u_+[n]|, |u_-[n]|\right)$$
$$= \frac{|u_+[n]| + |u_-[n]| + |(|u_+[n]| - |u_-[n]|)|}{2}. \tag{11}$$

The magnitudes of the errors $e[n]$ are less than or equal to the maximum uncertainty magnitudes, $u_{max}[n]$, so their summed energy will also be less than or equal to u_{mss}, the summed energy of $u_{max}[n]$

$$u_{mss} = \sum_{n=0}^{M-1} (u_{max}[n])^2 \geq \sum_{n=0}^{N-1} |e[n]|^2. \quad (12)$$

The summed time-domain energy of the sampled error waveform can be related to the energy in its DFT, $E[k]$, using Parseval's Theorem for the DFT [12]

$$\sum_{n=0}^{M-1} |e[n]|^2 = \frac{1}{M} \sum_{k=-M/2+1}^{M/2} |E[K]|^2. \quad (13)$$

Expressions (12) and (13) result in a bound on $|E[k]|$, even in the worst case, where all the error energy is concentrated in only one frequency component

$$|E[k]| \leq$$
$$\begin{cases} \sqrt{\dfrac{M \cdot u_{mss}}{2}} & \text{for } k = \pm 1, \pm 2, \cdots, \pm\left(\dfrac{M}{2} - 1\right), \\ \sqrt{M \cdot u_{mss}} & \text{for } k = 0, \pm\dfrac{M}{2}. \end{cases}$$
$$(14)$$

Since we want the error bounds on our estimate of the frequency response, which is the *CTFT* of the *derivative* of the step response, we have to both normalize as in (9) and account for the differentiation, by multiplying the bound determined in (14) by T and by $|j2\pi f_k| = |2\pi k/MT|$

$$V_{\|P+}(f_k) = -V_{\|P-}(f_k)$$
$$= \begin{cases} \left|\dfrac{2\pi k}{M}\right| \sqrt{\dfrac{M \cdot u_{mss}}{2}}, \\ \quad \text{for } k = \pm 1, \pm 2, \cdots, \pm\left(\dfrac{M}{2} - 1\right), \\ \left|\dfrac{2\pi k}{M}\right| \sqrt{M \cdot u_{mss}}, \\ \quad \text{for } k = 0, \pm\dfrac{M}{2}. \end{cases}$$
$$(15)$$

$V_{\|P+}(f_k)$ and $V_{\|P-}(f_k)$ are the positive and negative "Parseval" magnitude response uncertainty bounds, respectively, (the subscripted $\|$ symbol denotes magnitude) before correction for end effects.

B. Envelope-Modulation Method

The envelope-modulation bounding method was originally developed empirically, by bounding of the assumed worst-case errors: square waves that are offset and amplitude-modulated so as to just fit within the given uncertainties $u_-[n]$ and $u_+[n]$, as shown in Fig. 2. The assertion that such modulated square waves would produce the largest frequency-domain errors was based on two considerations. First, it seems apparent that the greatest frequency-domain errors will occur when the time-domain error waveform is periodic, concentrating the spectral energy into a small number of harmonic frequencies. Second,
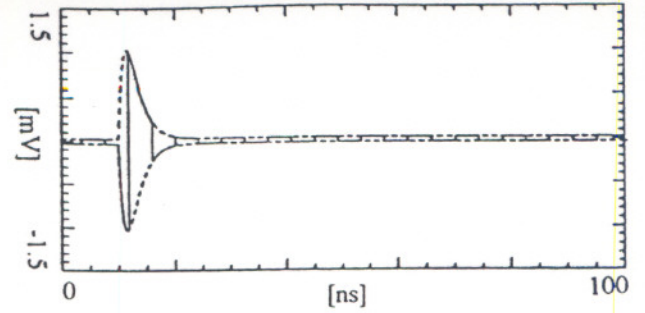

Fig. 2. An example of a possible worst-case error waveform, $-e(t)$: a square wave that is amplitude-modulated and offset (solid) so as to just fit within the uncertainty bounds $u_+(t)$ and $u_-(t)$ (dotted).

of all periodic signals having a fixed peak amplitude a, square waves contain the largest single spectral component (i.e., the fundamental sine component, having spectral amplitude of $4a/\pi$).

To determine the envelope-modulation bounds, we first calculate the average of the uncertainties, $u_{av}[n]$, and their halved difference, $u_{hd}[n]$

$$u_{av}[n] = \frac{u_+[n] + u_-[n]}{2}, \quad (16)$$

$$u_{hd}[n] = \frac{u_+[n] - u_-[n]}{2}. \quad (17)$$

A possible worst-case modulated-square-wave error, $e_{f,\theta}[n]$, is thus

$$e_{f,\theta}[n] = -u_{av}[n] - u_{hd}[n] \cdot q_{f,\theta}[n] \quad (18)$$

where $q_{f,\theta}[n]$ is a square wave with levels $+1$ and -1, frequency f, and phase θ. At $f = 0$, $q_{f,\theta}[n]$ is a dc level of $+1$ or -1. The DFT of $e_{f,\theta}[n]$ is

$$E_{f,\theta}[k] = -U_{av}[k] - U_{hd}[k] \circledast Q_{f,\theta}[k] \quad (19)$$

where $\circledast$ denotes circular convolution [13], and $U_{hd}[k]$ and $U_{av}[k]$ are the DFT's of $u_{hd}[n]$ and $u_{av}[n]$, respectively. Convolutions such as (19) are complicated, due to aliasing and the nature of the spectra of square waves. Note that the square-wave frequencies, f, are not required to be DFT bin center frequencies, f_k. Consider an example of uncertainties $u_-[n]$ and $u_+[n]$, and one possible worst-case error $e_{f,\theta}[n]$ shown in Fig. 2. For simplicity, the uncertainties are symmetric and $u_{av}[n] = 0$ in this example. The worst-case magnitude errors found using (19), over many tested values of f and θ, are shown by the solid curve in Fig. 3.

For all examples of uncertainty sets, $u_-[n]$ and $u_+[n]$ and errors, $e_{f,\theta}[n]$, tested by us, an upper bound on the frequency-domain error magnitudes, $|E_{f,\theta}[k]|$, was found to be $|U_{hd}[0]| + |U_{av}[k]|$

$$\max_{f,\theta} (|E_{f,\theta}[k]|) \leq |U_{hd}[0]| + |U_{av}[k]|. \quad (20)$$

This empirically-determined bound equation was then assumed to apply to all possible errors. For the last example, the bound is shown by the dotted curve in Fig. 3.

In fact, (20) has recently been mathematically proven [14] to bound all possible frequency-domain error magnitudes, $|E[k]|$
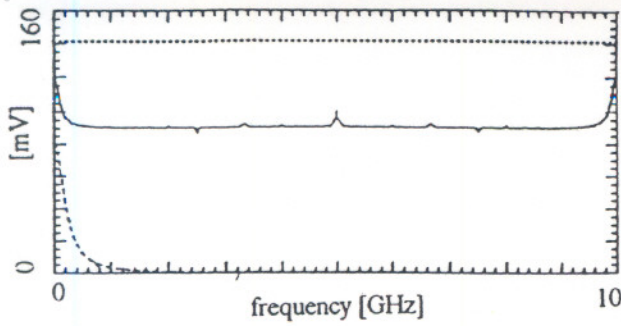
Fig. 3. Maximum magnitude response errors (solid), for amplitude-modulated square-wave errors of many tested frequencies and phases, that fit the uncertainties shown in Fig. 2. Also shown is $|U_{hd}[k]|$ (dashed), and the bound on the magnitude errors, $|U_{hd}[0]|$ (dotted). Frequency range is up to Nyquist ($1/2T$).
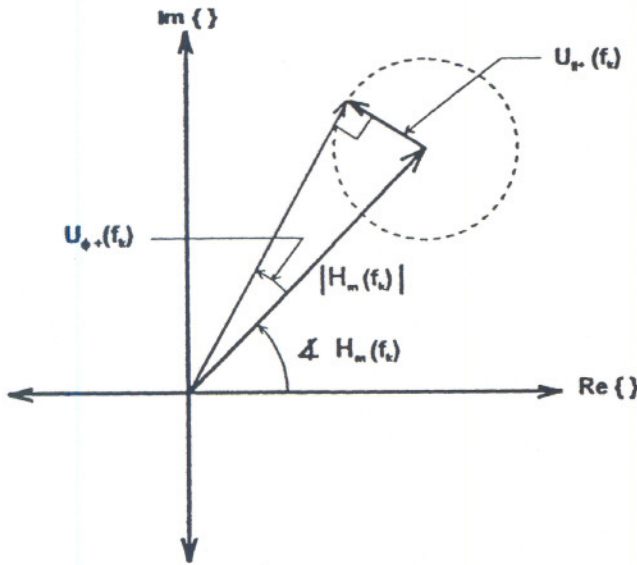

Fig. 4. Phasor diagram showing relationship of phase response uncertainty bound, $U_{\phi+}(f_k)$, to magnitude response uncertainty bound, $U_{||+}(f_k)$, and estimated frequency response $H_m(f_k)$.

The proof was given to us too close to press time, but it will be provided in a future paper.

As with the Parseval bounds, we multiply the bound determined in (20) by $|j2\pi f_k|$ and also by T

$$V_{||e+}(f_k) = -V_{||e-}(f_k)$$
$$= \left|\frac{2\pi k}{M}\right| (|U_{hd}[0]| + |U_{av}[k]|),$$
$$\text{for} \quad k = 0, \pm 1, \pm 2, \cdots, \pm \frac{M}{2}. \quad (21)$$

$V_{||e+}(f_k)$ and $V_{||e-}(f_k)$ are thus the positive and negative "envelope-modulation" magnitude response uncertainty bounds, respectively, before correction for end effects.

C. End Effects Corrections

The preceding sections make use of DFT's, and use multiplication by $|j2\pi f| = (2\pi k/MT)$ to correspond to differentiation. Underlying these processes is the implicit assumption that the error sequence $e[n]$ is M-periodic, e.g., $e[0] =$

$e[M]$, $e[1] = e[M+1]$, etc. However, $e[n]$ and its derivative are generally aperiodic. In order for the derivative of $e[n]$ to be made M-periodic, an impulse of amplitude equal to $(|e[M] - e[0]|)/T$ would have to be added to it. The maximum amplitude of such an impulse would be $\Delta_{\max}/T$, where

$$\Delta_{\max} = \max \{|(u_+[M] - u_-[0])|, |(u_-[M] - u_+[0])|\}. \quad (22)$$

Such an impulse is impossible to add in practice since $e[n]$ and its derivative are unknown. Thus, the frequency-domain bounds of (15) and (21) have to be expanded by $\Delta_{\max}$ at all values of k. Therefore, the Parseval and envelope-modulation magnitude uncertainty bounds, adjusted for end effects, are $U_{||P\pm}(f_k)$ and $U_{||e\pm}(f_k)$, respectively

$$U_{||P+}(f_k) = -U_{||P-}(f_k)$$
$$= \begin{cases} \left|\dfrac{2\pi k}{M}\right| \sqrt{\dfrac{M \cdot u_{mss}}{2}} + \Delta_{\max}, \\ \quad \text{for } k = \pm 1, \pm 2, \cdots, \pm\left(\dfrac{M}{2} - 1\right), \\ \left|\dfrac{2\pi k}{M}\right| \sqrt{M \cdot u_{mss}} + \Delta_{\max}, \\ \quad \text{for } k = 0, \pm \dfrac{M}{2}. \end{cases} \quad (23)$$

$$U_{||e+}(f_k) = -U_{||e-}(f_k)$$
$$= \left|\frac{2\pi k}{M}\right| (|U_{hd}[0]| + |U_{av}[k]|) + \Delta_{\max},$$
$$\text{for} \quad k = 0, \pm 1, \pm 2, \cdots, \pm \frac{M}{2}. \quad (24)$$

D. Phase Uncertainties

Corresponding phase uncertainty bounds can be calculated from the magnitude uncertainty bounds by assuming that error having magnitude equal to the magnitude uncertainty bound might be added to $H_m(f_k)$ so as to maximally change its phase. The phase uncertainty bounds are thus

$$U_{\phi\pm}(f_k) = \sin^{-1}\left[\frac{U_{||\pm}(f_k)}{|H_m(f_k)|}\right]. \quad (25)$$

This relationship is illustrated in Fig. 4.

IV. EXAMPLE

A simulation example is useful to illustrate time-domain uncertainties and how these methods transfer them to the frequency domain. Fig. 5 shows a hypothetical measured step-like waveform $s_m[n]$ having amplitude of 1 V and ~500 ps transition duration. The systematic uncertainties assigned to the measured waveform allow for a possible 1% overshoot in the true waveform, plus a decaying settling uncertainty of about 3 ns, and a constant uncertainty of 100 μV (0.01%) out to the end of the record, to model typical digitizer systematic uncertainties. The simulation sample interval is 50 ps, and the record size is 2 000 samples. Fig. 6 shows the resulting magnitude response estimate, $|H_m(f_k)|$, and phase response estimate, $\angle H_m(f_k)$, and their corresponding Parseval and envelope-modulation uncertainty bounds, calculated by the methods of Section III. For clarity, the phase $\angle H_m(f_k)$ has
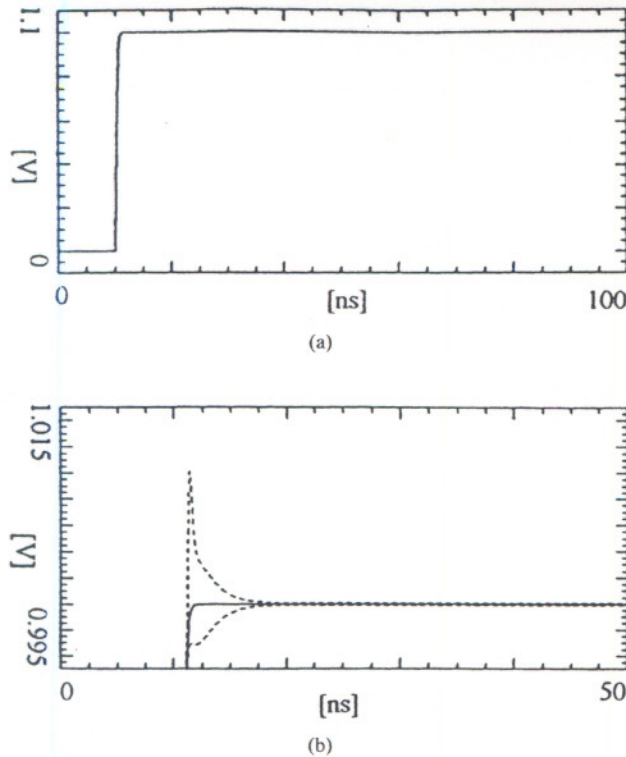
Fig. 5. (a) Simulated measured step-like waveform $s_m[n]$, and (b) the top portion of $s_m[n]$ (solid), with uncertainty envelope (dashed). Note the different scales for (a) and (b).
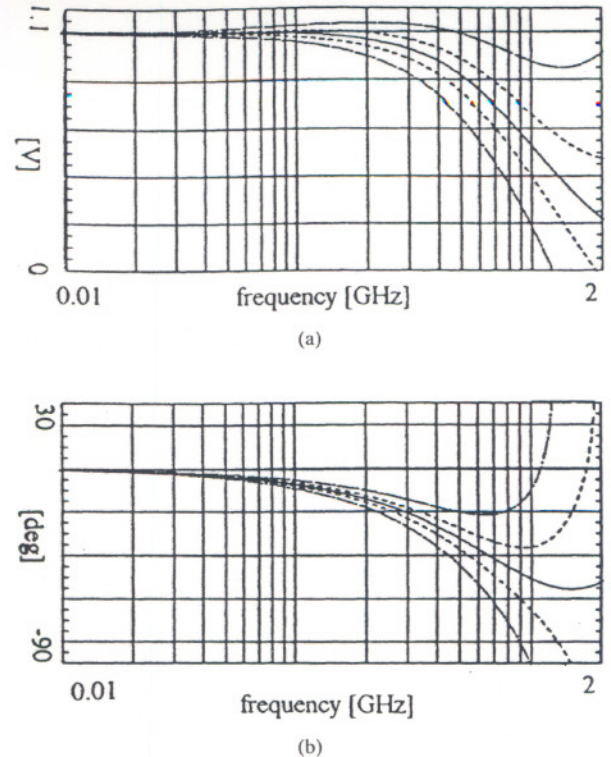

Fig. 6. Simulation results showing (a) the magnitude response estimate (solid), with envelope-modulation (dashed) and Parseval (dot-dashed) uncertainty bounds added; and (b) the unwrapped phase response estimate (solid) with its corresponding uncertainty bounds added (dashed, dot-dashed).

been unwrapped, and the linear (delay) part subtracted, as in [2].

Even for the moderate amount of time-domain uncertainty in this example, the magnitude and phase response uncertainties are significant at higher frequencies. Significant amounts of the magnitude and phase response uncertainties are contributed by the low-level ($100\,\mu$V) constant time-domain uncertainty, which allows for the possibility of significant narrowband error energy. Note also that as the magnitude response rolls off, the phase uncertainties become large, as expected from consideration of (25) and Fig. 4.

The Parseval bounds are very conservative (wide) for this example, in part because they do not account for the short-duration nature of most of the time-domain uncertainty.

V. APPLICATION

A practical application for the bounds on $H_m(f_k)$ developed above is in determining the uncertainties of estimating the frequency response, $H_D(f)$, of a separate device under test (DUT), *using $s_a(t)$ as the test input to the DUT.* Consider the case where $s_a(t)$ is the output of a step-like waveform generator, as suggested in Fig. 1(a). Let $s_{Da}(t)$ be the output of the DUT when $s_a(t)$ is the input to the DUT. Assume for simplicity that $s_{Da}(t)$ is somehow measured and sampled with perfect accuracy, with sampling interval T

$$s_{Da}[n] = s_{Da}(nT). \qquad (26)$$

(If this assumption is not valid, the additional measurement uncertainties can be incorporated.) Let $H_{Da}(f_k)$ be the DFT

of the derivative of $s_{Da}[n]$, normalized by T as in (9). Deconvolution of $H_m(f_k)$ from $H_{Da}(f_k)$ results in $H_{Dd}(f_k)$, the estimate of $H_D(f_k)$ (e.g., [15]). Sophisticated deconvolution algorithms may be required (e.g., [5]); if so, the uncertainties found earlier for $H_m(f_k)$ can be propagated through such algorithms (by magnitude division and phase subtraction) to find the corresponding uncertainties of $H_{Dd}(f_k)$. However, if $s_m(t)$ has a much shorter transition duration and settling time than $s_{Da}(t)$, then throughout the known flat region of $|H_m(f_k)|$ where $|H_m(f_k)| + U_{\|\pm}(f_k) \approx |H_m(0)|$, it may be valid to use very simple deconvolution to find $H_{Dd}(f_k)$, e.g., magnitude division and phase subtraction of $H_{Da}(f_k)$ by $H_m(f_k)$. In that case, to first order, the uncertainty bounds on $H_{Dd}(f_k)$ are equal to the uncertainty bounds on $H_m(f_k)$.

VI. CONCLUSIONS

The Parseval bounds are typically very conservative. Only in the unlikely case of uniform time-domain uncertainties (i.e., constant uncertainty for all n), is it even possible for the error energy to be concentrated into just one frequency. The envelope-modulation bounds are tighter, since they account for the shape of the time-domain uncertainties, but generally are still conservative, because the actual errors probably do not resemble modulated square waves. But it is important to note that certain error sources do have square-wave type characteristics. For example, gain and offset mismatch of interleaved samplers in certain digital oscilloscopes or waveform recorders can cause square-wave error patterns. If such an instrument is used to measure $s_m[n]$, then much of the error

energy could be concentrated at a single frequency. Pickup of clock signals or harmonics of power line frequencies can also produce significant errors at single frequencies. If persistent error tones occur, the relative size of the resulting frequency-domain error increases directly with the time duration of the recorded step-like waveform. Thus, time-domain uncertainty bounds that do not decay over time will produce increasingly large frequency-domain uncertainties as the recorded duration increases, because such uncertainties allow for the possibility of persistent error tones.

Obviously, great care should be taken in making the time-domain measurements, and setting the time-domain bounds as tightly as the measurements justify. The subject of setting time-domain bounds correctly is a significant problem for future research. It is worth repeating that the uncertainties developed here are best used for systematic errors only, and should be combined with those due to any separated random uncertainties, as well as those due to aliasing and differentiation errors, to produce total uncertainties.

An application of the uncertainties developed here is in finding the uncertainties of DUT frequency responses estimated by using the step-like signal $s_a(t)$ as the test input to the DUT's. A final note is that the methods applied here to uncertainties of step responses can be modified for application to uncertainties of impulse responses.

ACKNOWLEDGMENT

REFERENCES

[1] G. D. Cormack and J. O. Binder, "The extended function fast Fourier transform (EF-FFT)," *IEEE Trans. Instrum. Meas.*, vol. 38, no. 3, pp. 730–735, June 1989.
[2] T. M. Souders and D. R. Flach, "Accurate frequency response determinations from discrete step response data," *IEEE Trans. Instrum. Meas.*, vol. IM-36, no. 2, pp. 433–439, June 1987.
[3] J. J. Blair, "Error estimates for frequency responses calculated from time-domain measurements," submitted for publication to *IEEE Trans. Instrum. Meas.*
[4] W. L. Gans and J. R. Andrews, "Time domain automatic network analyzer for measurement of RF and microwave components," National Bureau of Standards, Boulder, CO, Tech. Note 672, Sept. 1975.
[5] W. L. Gans, "Dynamic characterization of waveform recorders and oscilloscopes using pulse standards," *IEEE Trans. Instrum. Meas.*, vol. 39, no. 6, pp. 952–957, Dec. 1990.
[6] O. B. Laug and T. M. Souders, "A custom integrated circuit comparator for high-performance sampling applications," *IEEE Trans. Instrum. Meas.*, vol. 41, no. 6, pp. 850–855, Dec. 1992.
[7] IEEE Standard 1057-1994, "IEEE Standard for Digitizing Waveform Recorders," pp. 42–43, Dec. 1994.
[8] W. L. Gans and N. S. Nahman, "Continuous and discrete Fourier transforms of steplike waveforms," *IEEE Trans. Instrum. Meas.*, vol. 31, no. 2, pp. 97–101, June 1982.
[9] A. V. Oppenheim and R. W. Schafer, *Digital Signal Processing*. Englewood Cliffs, NJ: Prentice-Hall, 1975, pp. 27, 98–100.
[10] L. R. Rabiner and K. Steiglitz, "The design of wide-band recursive and nonrecursive digital differentiators," *IEEE Trans. Audio Electroacoust.*, vol. AU-18, no. 2, pp. 204–209, June 1970.
[11] B. N. Taylor and C. E. Kuyatt, "Guidelines for evaluating and expressing the uncertainty of NIST measurement results," NIST Technical Note 1297, Sept. 1994.
[12] A. V. Oppenheim and R. W. Schafer, op. cit., p. 125.
[13] ———, op. cit., pp. 105–110.
[14] J. J. Blair, E.G.&G. Energy Measurements, Inc., private communication, Apr. 1995.
[15] T. M. Souders et al., "Characterization of a sampling voltage tracker for measuring fast, repetitive signals," *IEEE Trans. Instrum. Meas.*, vol. IM-36, no. 4, pp. 956–960, Dec. 1987.

John P. Deyst received the B.S. and M.S. degrees in electrical engineering from the Massachusetts Institute of Technology, Cambridge, in 1988 and 1990, respectively.

Since 1993, he has worked at the U.S. National Institute of Standards and Technology, Gaitherburg, MD, on characterizing waveform sampling and digitizing systems.

Mr. Deyst serves on the IEEE TC-10 Waveform Measurements and Analysis Committee.
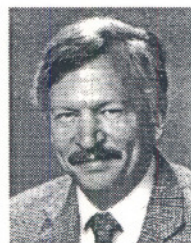
T. Michael Souders (M'75–SM'90–F'94) received the B.S. degree in physics from Johns Hopkins University, Baltimore, MD, in 1967.

Since that time, he has been a career employee with the National Institute of Standards and Technology, Gaithersburg, MD. His primary interests in recent years include standards and test methods for data acquisition and conversion devices, and efficient testing strategies for complex systems. He has published more than 30 articles on work in these fields.

Mr. Soulders serves as Chairman of the IEEE Waveform Measurements and Analysis Committee.